A Study of FR2 Radio Propagation with Focus on Mobility Management in an Industrial Scenario

Ramírez Arroyo, Alejandro; Lechuga, Melisa Maria Lopez; Rodriguez, Ignacio; Sørensen, Troels Bundgaard; Caporal Del Barrio, Samantha; Valenzuela-Valdes, Juan F. ; E. Mogensen, Preben

Published in:
17th European Conference on Antennas and Propagation, EuCAP 2023

DOI (link to publication from Publisher):
10.23919/EuCAP57121.2023.10132940

Publication date:
2023

Document Version
Accepted author manuscript, peer reviewed version

A Study of FR2 Radio Propagation with Focus on Mobility Management in an Industrial Scenario

Alejandro Ramírez-Arroyo*, Melisa López†, Ignacio Rodríguez‡, Troels B. Sørensen†,
Samantha Caporal del Barrio§, Juan F. Valenzuela-Valdés*, Preben Mogensen†,§
*Department of Signal Theory, Telematics and Communications, University of Granada (CITIC-UGR), 18071 Granada, Spain;
(e-mails: alera@ugr.es; juanvalenzuela@ugr.es)
†Department of Electronic Systems, Aalborg University (AAU), 9220 Aalborg, Denmark;
(e-mails: mll@es.aau.dk; tbs@es.aau.dk; pm@es.aau.dk)
‡Department of Electrical Engineering, University of Oviedo (UNIOVI), 33203 Gijón, Spain;
(e-mail: irl@uniovi.es)
§Nokia, 9220 Aalborg, Denmark;
(e-mail: samantha.caporal_del_barrio@nokia-bell-labs.com)

***Abstract*—This work presents the analysis of a measurement campaign performed in a realistic two-hall industrial environment for FR2 band. In order to provide secure, reliable and high available Machine-to-Machine communications in the mmWave band for Industrial Internet of Things mobile applications, a study of the physical propagation channel must be carried out. The analysis shows the high variability of the propagation channel depending on the Line-of-Sight or Non Line-of-Sight condition, with path loss exponents ranging from 2.10 to 4.56. The mobility analysis demonstrates the high probability of beam switching if a threshold is not defined. By imposing this threshold, there is a decrease in the complexity of mobility management in exchange for a reduction in received power at the end user.**

***Index Terms*—channel model, factory, mmWave, mobility management, path gain, propagation.**

I. Introduction

In recent years, telecommunications are moving towards the new fifth-generation (5G) standard. The main focus of this new generation is the improvement of Key Performance Indicators (KPIs) (e.g., throughput, end-to-end latency or energy consumption) with respect to previous generations, thus improving the end-user experience and providing service for different use cases with different KPI requirements [1], [2]. One of these new scenarios is the case of factories for Industrial Internet of Things (IIoT) applications. Industry 4.0 aims to fully automate the production process in factories. This requires autonomous agents capable of coordinating in heterogeneous conditions [3], [4]. In this environment, in addition to the previously mentioned KPIs, reliability and availability become fundamental for the correct operation of the industry [5], [6].

The main objective of this paper is to present a measurement campaign performed in an industrial environment, where typical conditions of a factory are fulfilled, i.e, indoor scenario with high ceilings, presence of dense clutter of production machinery and a multi-path effect accentuated by the presence of metallic objects [7]. While the use of sub-6 GHz/FR1 bands has been widely studied in industrial environments [8], [9], the use of mmWave/FR2 bands provides new opportunities. mmWave frequencies in indoor environments are expected to be fundamental due to increased bandwidth availability [10]. Despite the higher attenuation in this frequency range, the use of antennas with high directivities and large antenna arrays together with beam switching, aim to provide full coverage to the end user [11]. Thus, the characterization of the propagation channel and the analysis of the mobility management turn crucial. Optimal resource management is able to provide secure and reliable Machine-to-Machine (M2M) communications in factory environments [12].

This work is organized as follows. Section II presents the industrial scenario where the measurements have been performed and the experimental setup. Section III discusses some results related to the propagation channel model and mobility management. Finally, Section IV draws the main results of the work.

II. Experimental scenario and setup

This section presents the experimental setup and the industrial scenario where the measurement campaign has been performed. The measurement data were obtained in the AAU 5G Smart Production Lab, located in Aalborg, Denmark. The lab is composed of two halls, and has a total area of 1250 m^2. The environment resembles a real manufacturing and production environment, including elements such as production line modules, Autonomous Mobile Robots (AMRs) and robotic arms [13]. These characteristics result in a favorable environment for multipath propagation due to the reflection off metallic interfaces. Fig. 1 shows an overall view of the lab, where a dense clutter environment can be depicted.

A Nokia 5G Airscale mmWave Radio module acting as TX [14] is located at a height of 3 meters in the main hall of the lab (see Fig. 1). This TX operates in the n258 mmWave/FR2 band (24.25-27.5 GHz) with carrier bandwidth up to 600 MHz. The module configuration provides 32 beams

Fig. 1. View of the AAU 5G Smart Production Lab. The transmitter module (TX) is located on the left side. The scanner and the receiver antenna (RX) are located on the AMR system.

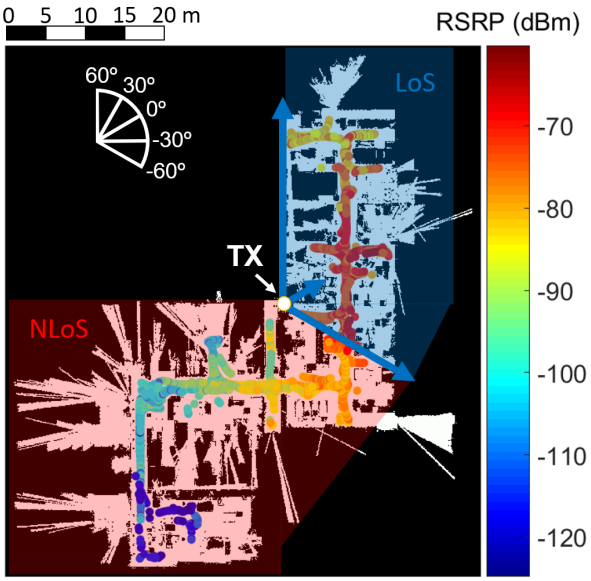

Fig. 2. Maximum RSRP received at each position in the laboratory. Due to the location and orientation of the transmitter module, two propagation zones are considered: LoS (blue) and NLoS (red). The horizontal coverage angles are shown in the upper left corner.

with $\pm 60°$ horizontal coverage and gains up to 23.9 dBi. Considering the location and horizontal coverage of the TX, the laboratory is divided into two zones according to the beam coverage; Line-of-Sight (LoS) and Non-Line-of-Sight (NLoS) regions (see Fig. 2). Additionally, vertical coverage allows downtilt, i.e., elevation angles, range from 0° to 17°.

The measurement acquisition process is performed using a Rohde & Schwarz TSME6 Drive Test Scanner [15], which measures the Reference Signal Received Power (RSRP) for each Synchronization Signal Block (SSB) transmitted by each of the 32 beams. This scanner is connected to a receiver (RX) biconical antenna (Model: #SZ-3004000/P) [16] located at a height of 1.5 meters above the ground (as shown in Fig. 1). The radio network scanner is placed on top of an AMR MiR200 [17], holding the biconical antenna with the grip of a robotic manipulator. By defining specific routes to be followed by the AMR, the scanner is able to measure RSRP values along the main corridors in the lab. The robot moves at an average speed of 1.5 $\mathrm{m/s}$. The position of the AMR is obtained at all points in the route by using its built-in Simultaneous Localization And Mapping (SLAM) algorithm, which is based on a calibrated reference system and the information provided by the onboard Light Detection And Ranging (LiDAR) system resulting in cm-level accuracy. In total, 212330 samples are obtained over a period of 6768 s, where at least one SSB is reachable at each timestamp. All SSBs from each of the 32 beams are observed in 48.9% of the recorded samples.

III. Industrial Scenario Analysis

In order to provide optimal cellular service in industrial environments, a physical characterization of the scenario must be performed. This section presents an analysis of path gain propagation in LoS and NLoS regions, and mobility aspects that may be considered in an industrial environment, such as beam switching. Fig. 2 shows the maximum RSRP observed at all RX locations measured in the lab. The figure suggests that there are mainly two factors that affect the RSRP: the TX-RX link distance and the LoS/NLoS condition. RX positions close to the TX achieve RSRP values of up to -62 dBm, while the RSRP on those locations far from the TX module are attenuated due to channel propagation. Additionally, the NLOS region presents higher RSRP attenuation in terms of distance.

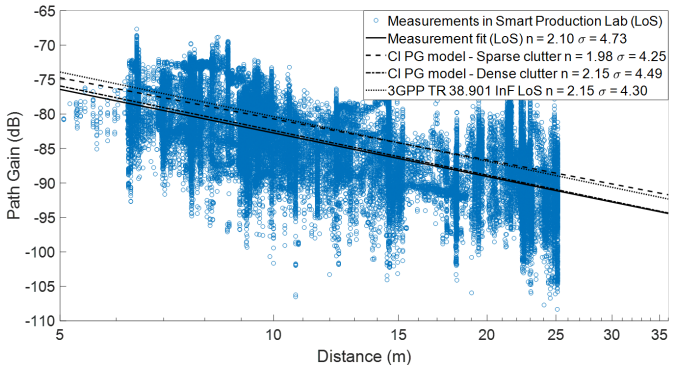

Fig. 3. LoS path gain measurements and model fits.

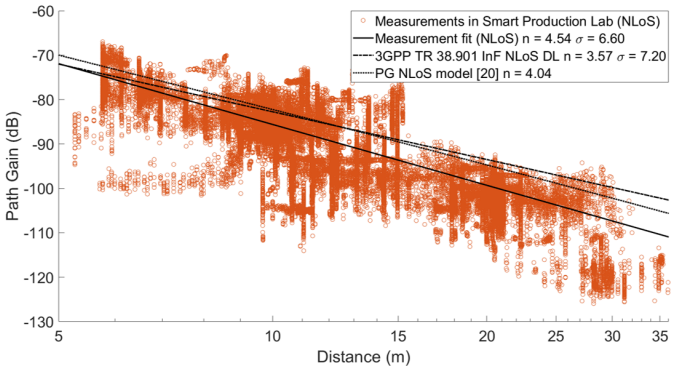

Fig. 4. NLoS path gain measurements and model fits.

A. Path Gain

To quantify the impact of LoS and NLoS in the factory, the Path Gain (PG) of the propagation channel is calculated as:

$$PG[\text{dB}] = RSRP[\text{dBm}] - [P_{TX,SC}[\text{dBm}] + G_{TX}(\phi,\theta)[\text{dBi}] + G_{RX}(\phi,\theta)[\text{dBi}]] \quad (1)$$

$$P_{TX,SC}[\text{dBm}] = P_{TX}[\text{dBm}] - 10 \cdot \log 10(B_T/B_{SC}) \quad (2)$$

where $G_{TX}(\phi,\theta)$ and $G_{RX}(\phi,\theta)$ stand for the TX and RX antenna gain in azimuth and elevation angles, respectively. P_{TX} is the total power transmitted over the entire bandwidth B_T, and $P_{TX,SC}$ is the power transmitted in the subcarrier (SC) bandwidth, i.e., B_{SC}. For this specific study, $P_{TX,SC} =$ 21.2 dBm, $B_T = 100$ MHz and $B_{SC} = 120$ kHz for the TX configuration used during the measurements.

The path gain in terms of distance can be modeled as a slope-intercept model as:

$$PG(d) = PG_{1m} - 10n \cdot \log 10(d) + \mathcal{N}(0,\sigma^2) \quad (3)$$

where PG_{1m} is the path gain at 1 m distance, n represents the path loss exponent and $\mathcal{N}(0,\sigma^2)$ is a normal distribution with standard deviation σ that models the propagation channel shadow fading effect.

Fig. 3 shows the path gain versus the distance for LoS in the factory. The measurement fit for LoS data provide $PG_{1m} = -61.73$ dB, $n = 2.10$, $\sigma = 4.73$ dB. This model is compared to the close-in free space (CI) path-loss models for sparse and dense clutter in factories [18], and 3GPP TR 38.901 Indoor Factory (InF) LoS model [19], both shown in Fig. 3. In order to compare the previous models with the measurement fit, the root mean square error (RMSE) is calculated between the measurement data and the slope-intercept models. A good agreement is found if RMSE is closely related to σ. RMSE values are 5.21 dB, 4.73 dB and 5.27 dB for CI sparse clutter, CI dense clutter and 3GPP InF LoS models, respectively. Note that $\sigma = 4.49$ dB in the dense clutter case, closely related to the best fit obtained RMSE of 4.73 dB, showing a good match between the measurements and the model. Fig. 4 presents the path gain in terms of distance for NLoS paths. The fit parameters are $PG_{1m} = -40.11$ dB, $n = 4.54$, $\sigma = 6.60$ dB. Fig. 4 also shows the 3GPP TR 38.901 Indoor Factory (InF) NLoS DL model [19] and the the theoretical NLoS path gain model developed in [20] with ceiling height $h_{ceil} = 5$ m and clutter height $h_{clut} = 2.5$ m. RMSE values for both models are 7.78 dB and 7.61 dB. Since $\sigma = 6.60$ dB for the measurement fit, a reasonable match is also found for NLoS data.

B. Beam coverage and mobility management

Due to the FR2 frequency range, the TX beams provide high directivity in this setup, and the best server SSB for RX service highly varies depending on the RX position. The presence of up to 32 beams is an advantage in case there is a serving beam failure. They give the possibility of beam failure recovery, by ensuring that there is a secondary beam that may act as serving in case of radio link failure. However, the high number of available beams with high directivity could lead to a high beam switching rate in the network. This is why the integration of management mechanisms is considered fundamental. Fig. 5 shows the cumulative distribution function for the difference (Δ) between the first and the second strongest RSRP SSBs. This metric can be defined as:

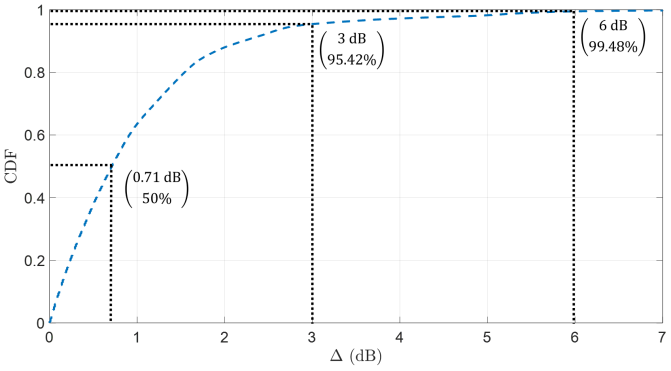

Fig. 5. CDF for the RSRP difference between the two beams with the highest RSRP.

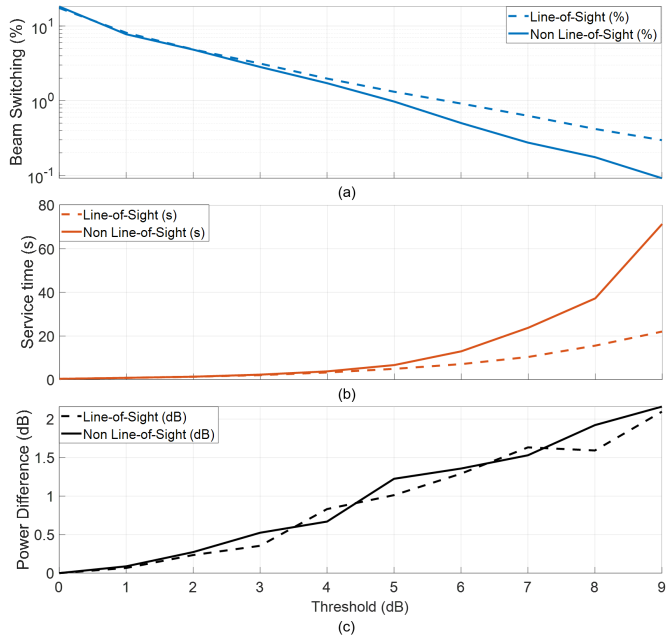

Fig. 6. a) Beam Switching probability, b) average beam service time and c) average beam power difference versus thresholds in LoS and NLoS paths. A 3th-order median filter is applied in the time series in order to smooth the shadow fading effect.

$$\Delta = RSRP_{1st\,SSB} - RSRP_{2nd\,SSB} \quad (4)$$

As shown, 50%, 95.42% and 99.48% of the time, a secondary SSB is available with a maximum decrease of 0.71 dB, 3 dB and 6 dB, respectively. These results confirm that beam failure recovery, which requires that the secondary beam is received with at least half of the power than the observed in the primary beam, is possible with 95% probability.

A well-functioning beam-recovery is a trade-off between availability and a high beam-switching rate (which may result in a poor resource management), i.e., high availability implies high beam switching rate. Therefore, the use of different beam switching thresholds is also studied, considering the trade-off between a continuous and reliable communication and an optimal radio resource and mobility management. Fig. 6 shows the impact of different beam switching thresholds to beam switching probability, average beam service time and average beam power lost due to a reduction in the beam switching rate. Beam switching applies if the following condition is met:

$$RSRP_{1st\,SSB} - RSRP_{serving\,SSB} > Threshold \quad (5)$$

Fig. 6(a) shows the beam switching probability for several values of threshold. When the threshold is not considered, i.e., 0 dB, the probability is about 18%. However, if threshold increases to 9 dB, this probability decreases to 0.30% (LoS) and 0.09% (NLoS). Since the number of available beams in NLoS paths is lower than in LoS paths due to the environment, the beam switching probability decreases faster for large threshold values. Fig. 6(b) presents the average service time per beam, which is calculated as:

$$t_{service}[\mathrm{s}] = \frac{t_{total}[\mathrm{s}]}{N_{samples} \cdot P(BS)} \quad (6)$$

where t_{total} stands for the entire period during which the measurements have been performed, $N_{samples}$ is the number of measured samples, and $P(BS)$ is the beam switching pobability. The service time increases with higher threshold values. This effect is accentuated for the NLoS cases due to the lower probability of beam switching. Fig. 6(c) shows the average power difference between the serving beam and the beam with the highest power. This power difference shows the average power loss due to the fact that the scanner is not

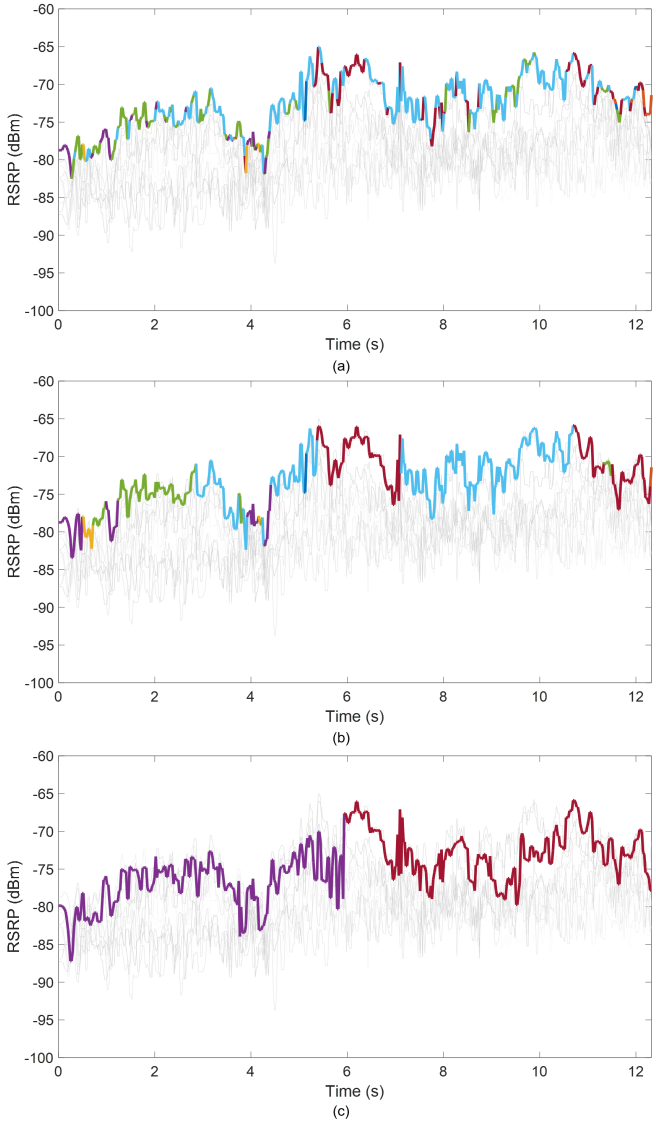

Fig. 7. Time series for the serving SSB in the LoS path for cases with (a) 0 dB, (b) 3 dB and (c) 10 dB threshold. RSRPs for those beams to which the scanner is not connected are marked in gray. A 3th-order median filter is applied in the time series in order to smooth the shadow fading effect.

being served by the best beam to decrease the beam-switching rate. In this case, the difference linearly increases in both LoS and NLoS regions. For a threshold value of 3 dB, an average of 0.5 dB is lost with respect to the available beam with maximum power. As a visual example of the previous mobility analysis, Fig. 7 illustrates a 12.3 second time series of the RX movement throughout the factory, where each color denotes a different serving beam through the time series and gray lines denote RSRP from beams which are not serving. This time series corresponds to a 9.2 meters movement from south to north across the main corridor in the LoS region (see Fig. 2). Fig. 7(a) achieves the highest RSRP at any time since the beam switching threshold is not applied. However, this results in 148 beam switches in the time series route. Fig. 7(b) applies a 3 dB threshold, which represents a serving RSRP loss of approximately 0.5 dB. In exchange, the number of beam switches has been reduced to 22. A conservative case in terms of beam switching is shown in Fig. 7(c), where a 10 dB threshold implies a single beam switching. In this case, RSRP is reduced by 2.1 dB on average. In summary, as statistically denoted in Fig. 6, in exchange for decreasing the beam switching phenomenon, the RSRP slightly decreases.

IV. Conclusion

In this paper, we study the characterization of the propagation channel in an industrial environment using measurement data from a realistic smart manufacturing environment. The analysis of the measurements shows RSRP values between -62 dBm and -125 dBm for distances between 2 and 36 meters in the FR2 frequency band (24.25-27.5 GHz). The high influence of the LoS and NLoS conditions in this type of environment has been demonstrated, going from a path loss exponent of $n = 2.10$ in LoS to $n = 4.54$ in NLoS. Finally, the mobility analysis shows that the use of a threshold reduces the beam switching probability in the network. An optimal performance may be achieved by selecting the beam switching threshold that best adapts to the environment or service conditions.

Acknowledgment

This work was partially supported by the Spanish Ministry of Science and Innovation under Ramon y Cajal Fellowship number RYC-2020-030676-I, and Predoctoral Grant FPU19/01251.

References

[1] L. Chettri and R. Bera, "A Comprehensive Survey on Internet of Things (IoT) Toward 5G Wireless Systems," *IEEE Internet of Things Journal*, vol. 7, no. 1, pp. 16-32, 2020.

[2] J. Zhang, E. Björnson, M. Matthaiou, D. W. K. Ng, H. Yang and D. J. Love, "Prospective Multiple Antenna Technologies for Beyond 5G," *IEEE Journal on Selected Areas in Communications*, vol. 38, no. 8, pp. 1637-1660, 2020.

[3] B. Chen, J. Wan, L. Shu, P. Li, M. Mukherjee and B. Yin, "Smart Factory of Industry 4.0: Key Technologies, Application Case, and Challenges," *IEEE Access*, vol. 6, pp. 6505-6519, 2018.

[4] S. Wang, J. Wan, D. Zhang, D. Li and C. Zhang, "Towards smart factory for Industry 4.0: a self-organized multi-agent system with big data based feedback and coordination," *Computer Networks*, vol. 101, pp. 158-168, 2016.

[5] E. Sisinni, A. Saifullah, S. Han, U. Jennehag and M. Gidlund, "Industrial Internet of Things: Challenges, Opportunities, and Directions," *IEEE Transactions on Industrial Informatics*, vol. 14, no. 11, pp. 4724-4734, 2018.

[6] N. Xia, H. -H. Chen and C. -S. Yang, "Radio Resource Management in Machine-to-Machine Communications—A Survey," *IEEE Communications Surveys & Tutorials*, vol. 20, no. 1, pp. 791-828, 2018.

[7] E. Tanghe, D. P. Gaillot, M. Liénard, L. Martens and W. Joseph, "Experimental Analysis of Dense Multipath Components in an Industrial Environment," in IEEE Transactions on Antennas and Propagation, vol. 62, no. 7, pp. 3797-3805, July 2014.

[8] W. Wang, S. L. Capitaneanu, D. Marinca and E. -S. Lohan, "Comparative Analysis of Channel Models for Industrial IoT Wireless Communication," *IEEE Access*, vol. 7, pp. 91627-91640, 2019.

[9] I. P. Guembe et al., "Wireless Characterization and Assessment of an UWB-Based System in Industrial Environments," *IEEE Access*, vol. 9, pp. 107824-107841, 2021.

[10] L. You et al., "Network Massive MIMO Transmission Over Millimeter-Wave and Terahertz Bands: Mobility Enhancement and Blockage Mitigation," *IEEE Journal on Selected Areas in Communications*, vol. 38, no. 12, pp. 2946-2960, 2020.

[11] M. Giordani, M. Polese, A. Roy, D. Castor and M. Zorzi, "A Tutorial on Beam Management for 3GPP NR at mmWave Frequencies," *IEEE Communications Surveys & Tutorials*, vol. 21, no. 1, pp. 173-196, 2019.

[12] A. Stamou, N. Dimitriou, K. Kontovasilis and S. Papavassiliou, "Autonomic Handover Management for Heterogeneous Networks in a Future Internet Context: A Survey," *IEEE Communications Surveys & Tutorials*, vol. 21, no. 4, pp. 3274-3297, 2019.

[13] I. Rodriguez et al., "5G Swarm Production: Advanced Industrial Manufacturing Concepts Enabled by Wireless Automation," *IEEE Communications Magazine*, vol. 59, no. 1, pp. 48-54, 2021.

[14] Nokia. (2022). *AirScale mmWave Radio*. [Online]. Available: https://www.nokia.com/networks/mobile-networks/airscale-radio-access/mmwave-radio/

[15] Rohde & Schwarz. (2022). *R&S TSME Drive Test Scanner*. [Online]. Available: https://www.rohde-schwarz.com/manual/r-s-tsme-drive-test-scanner-user-manual-manuals-gb1_78701-55041.html

[16] *SZ-3004000/P Bi-Conical Antenna 3-40* GHz. [Online]. Available: https://www.ainfoinc.com/amfilerating/file/download/file_id/4510/

[17] Mobile Industrial Robots. (2022). *MiR200*. [Online]. Available: https://www.mobile-industrial-robots.com/

[18] T. Jiang et al., "3GPP Standardized 5G Channel Model for IIoT Scenarios: A Survey," *IEEE Internet of Things Journal*, vol. 8, no. 11, pp. 8799-8815, 2021.

[19] "Study on channel model for frequencies from 0.5 to 100 GHz, v17.0.0," 3GPP, Sophia Antipolis, France, Rep. TR 38.901, 2022. [Online]. Available: https://portal.3gpp.org/desktopmodules/ Specifications/SpecificationDetails.aspx?specificationId=3173

[20] D. Chizhik et al., "Directional Measurements and Propagation Models at 28 GHz for Reliable Factory Coverage," *IEEE Transactions on Antennas and Propagation*, vol. 70, no. 10, pp. 9596-9606, Oct. 2022.